

Tribological Study of a Mechanical Component Built on a Benzine Engine Utilizing the Finished Elements Method (F.E.M.) And Coffin-Manson's Law

Vincenzo Niola, Giuseppe Vitale
Department of Mechanical Engineering for Energy of Naples
Federico II
Via Claudio 21, 80125
Napoli, ITALY

Abstract: In this paper, a model embedded-embedded beam with thermal gradient has been analyzed. In particular, a part of unloaded system car, denominated *hot end*, has been studied. This mechanical component is subject to hot gas flow (over 800°C) in some conditions and to lower hot gas flow (about 400°C) in others. So, there is a high thermal range, above all between extreme parts of component that results fixed in superior and inferior zone. Thermal gradient induces the growth of stresses and deformations in component, in particular near fixings. Repetitions of thermal cycles can determine a breaking due to thermal fatigue. According to Normative Fiat 7-A3760, *hot end* must resist at least to 1000 thermal cycles to can be validate in production. Knowing deformations in critical zones, it has been applied Coffin-Manson's law, obtaining breaking thermal cycles, that is thermal fatigue life. Three hypotheses have been considered: two are extreme cases, one is realistic case. All cases respect normative: *hot end* resists over 1000 thermal cycles.

Key-Words: - Tribology, Mechanics, Finished elements method, Materials .

1 Introduction

Unloaded system for a car is composed by two macro parts: a tract connected to propulsion denominated *hot end*, in which burnt gases pass to high temperatures (over 800°C). In the other, denominated *cold end*, gases pass to loss temperatures. The mechanical component more interesting to study is *hot end*, because it arrives to danger temperatures for its duration life. To have an idea about this mechanical component it can observe some next photos.



Fig. 1 – Mechanical component



Fig.2 – Hot end

In these photos two different sights of *hot end* are illustrated, without turbo compressor. In fact, fixing holes between turbo compressor and welded cone are visible; welded cone is connected to catalyst.

In cad model of *hot end* there is a part of turbo compressor, connected to cone.

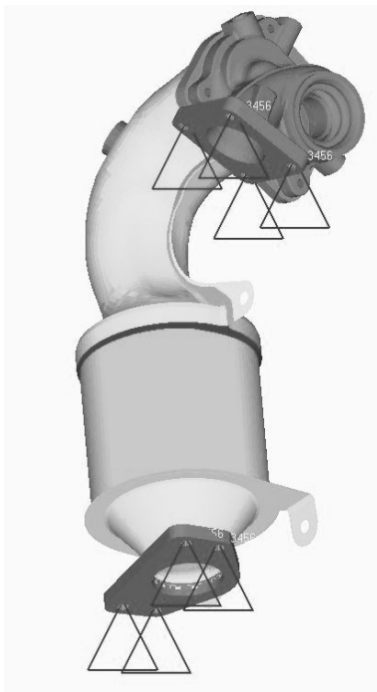


Fig. 3 - Hot End: Cad Model

Triangles represent fixings: in inferior zone flange is connected to *cold end*, in which gases are temperatures lower than precedent zone. This model represents a embedded-embedded beam with thermal gradient. Hot End: Cad Model.

2 Materials

The analyzed mechanical component is made with two different materials: iron cast for turbo compressor and ferritic steel *AISI 441* for

remaining part. These materials have the propriety to resist to high temperatures.

2.1 Iron Cast

Generally it is a ferrous alloy with a fusion temperature about 1150-1300°C.

Degree	Number UNS	Composition (%weight)	Traction resistance (MPa)	Yelding load (MPa)	Ductility (A% on 50 mm)
ASTM A536-45006	F22200	2.3-2.7 C 1.25-1.55 Si <0.55 Mn	345-448	224-310	6-10

Table 1: Iron Cast's Characteristics

2.2 Ferritic Steel AISI 441

C	Mn	Si	Ni	Cr	Nb	Ti	N	Al
<=0,025	<=0,4	<=0,5	<=0,50	7,5 19	>=0,3	0, 10 0,35	<=0,03	<=0,10

Table 2: Chemical Composition (%)

State of Supply	σ_R [N/mm ²]	Traction σ_S [N/mm ²]	Al A50 [%min.]	AI HRB [max.]
Cold Laminating	400-520	>=260	27	70:80
Hot Laminating	440-550	>=280	25	75:85

Table 3: Mechanical Characteristics

Density	7,72 kg/dm ³
E (20°C)	220.000 N/mm ²
k (20°C)	0,062 Cal/cm s °C

Table 4: Physical Characteristics

3 Simulative Procedure

According to Normative Fiat 7-A3760, *hot end* must resist to 1000 thermal cycles, as it can observe in next graphic (fig.4), taken by normative.

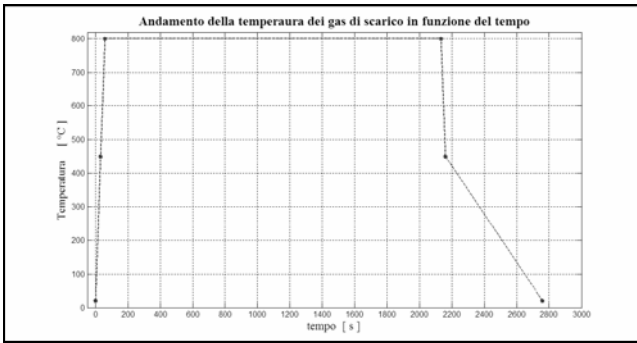


Fig. 4

In graphic temperature depending by time is reported. Burnt gas gets hot by environment temperature (about 20°C) until 800°C in a time range (taken by normative). After about 2000 seconds to 800°C, it gets cold in two steps, until to return to environment temperature. This cycle represents the maximum and the minimum power to which engine can arrives. To obtain N_f , that is breaking cycles number, it is necessary to consider some important events. When engine arrives to maximum power, it is possible to calculate *hot end's* maximum temperatures with Method of Finished Elements (F.E.M.). In particular, temperatures next to superior flange are considered, because they are highest temperatures. Then, this zone is the most dangerous to eventual material's breaking and so it is important to make an accurate analysis. When engine arrives to minimum power, it is possible to calculate *hot end's* minimum temperatures. These two temperature fields represent input data for a new calculation to obtain stress and deformation fields as output data.

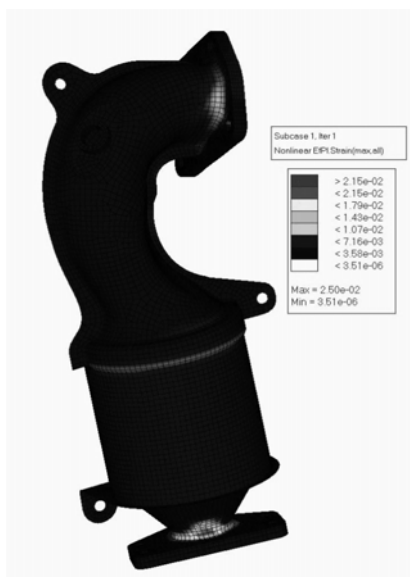


Fig. 5 Plastic Deformation Field for Maximum Temperatures

In Fig.5 there is *hot end* in post-processing, with plastic deformations due to maximum temperatures. In caption there are plastic deformations for all component; plastic deformations are greater near to flanges than the resting parts of component. In particular, it has been analyzed superior zone, because it is subject to highest temperatures (see Fig. 6).

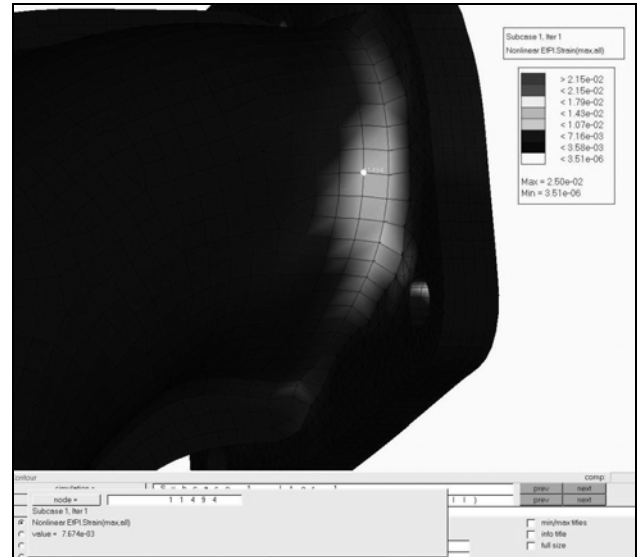


Fig. 6 *Hot End*: Superior Zone's Enlargement

As it can see in Fig. 6, the node N° 11494 is subject to highest plastic deformation, $\epsilon_{pl \max} = 7.67 \cdot 10^{-3}$. For the same node it is possible to calculate plastic deformation due to minimum temperatures, $\epsilon_{pl \min} = 3.94 \cdot 10^{-4}$. Since total deformation is sum of elastic and plastic deformation, it must know elastic component for two temperature fields. It is possible to calculate elastic deformation through elastic modulus value and Von Mises' stress for that node and to node's temperature. In next figures 6 and 7 there are superior zone's enlargements (in post-processing) for maximum and minimum temperature fields.

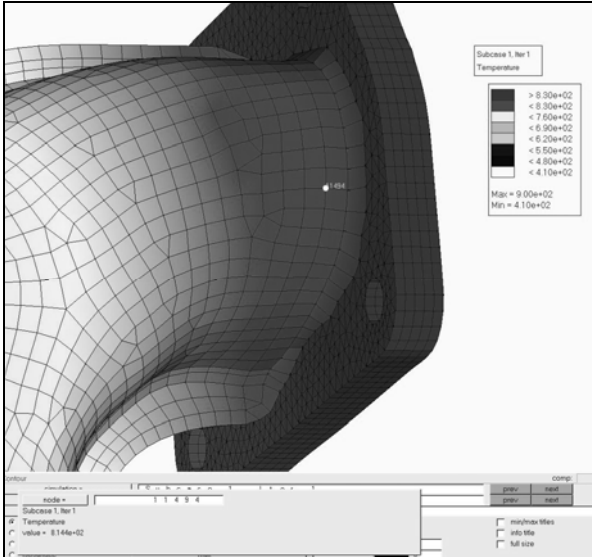


Fig. 7 Node N° 11494: temperature for maximum temperature field

In this node temperature is **812°C**, and **E (812°C) = 1,153*10¹¹ Pa.**

Total deformation calculation for maximum temperature field:

$$\epsilon_{el \max} = \sigma_{eq \text{ VM}} / E_{MAX} = 1,233 \cdot 10^8 \text{ Pa} / 1,153 \cdot 10^{11} \text{ Pa} = 1.070 \cdot 10^{-3}$$

$$\epsilon_{tot \max} = \epsilon_{pl \max} + \epsilon_{el \max} = 7.67 \cdot 10^{-3} + 1.070 \cdot 10^{-3} = 8,744 \cdot 10^{-3}$$

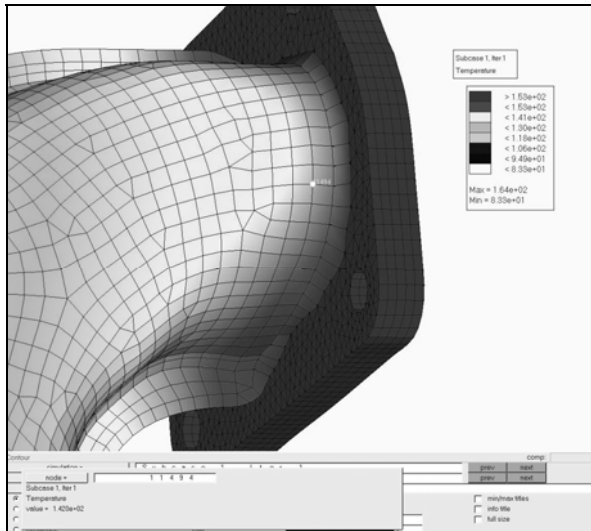


Fig. 8 Node N° 11494: temperature for minimum temperature field

In this node temperature is **142°C**, and **E (141°C) = 2.107*10¹¹ Pa.**

Total deformation calculation for minimum temperature field:

$$\epsilon_{el \min} = \sigma_{eq \text{ VM}} / E_{MIN} = 8.767 \cdot 10^7 \text{ Pa} / 2.107 \cdot 10^{11} \text{ Pa} = 4.161 \cdot 10^{-4}$$

$$\epsilon_{tot \min} = \epsilon_{pl \min} + \epsilon_{el \min} = 3.94 \cdot 10^{-4} + 4.161 \cdot 10^{-4} = 8.097 \cdot 10^{-4}$$

4 Coffin-Manson's Law

The strain life relationship is given by the following equation proposed by Coffin-Manson:

$$\frac{\Delta \epsilon}{2} = \frac{\Delta \epsilon_e}{2} + \frac{\Delta \epsilon_p}{2} = \frac{\sigma'_f}{E} (2N_f)^b + \epsilon'_f (2N_f)^c \quad (1)$$

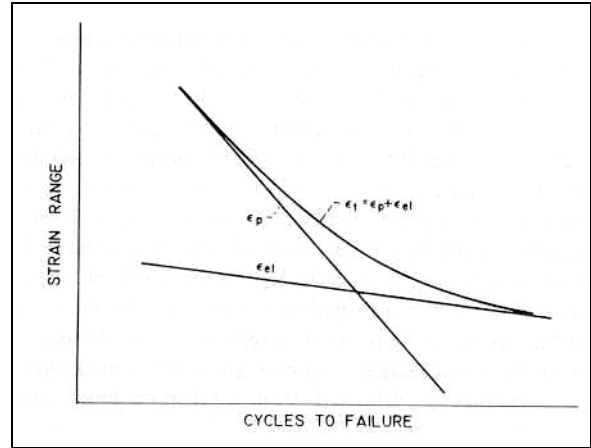


Fig. 9

where $\Delta \epsilon_f$ is total strain range, $2N_f$ is the number of reversals to failure, E is the elastic modulus, σ'_f is the fatigue strength coefficient, ϵ'_f is the fatigue ductility coefficient, b is the fatigue strength exponent and c is the fatigue ductility exponent.

5 Resultes

An important step in this simulation is to consider materials' characteristics depending by temperature. Some important physical greatnesses temperature's functions are:

- **k = k (T), thermal conductivity;**
- **α = α (T), thermal expansion coefficient;**
- **σ - ε (T), stress-deformation curve**

Appling Coffin-Manson's Law, knowing all coefficients about materials (in this case ferritic steel AISI 441), it can consider three cases.

5.1 Best Case

$\Delta \epsilon / 2$	N_f	σ'_f / E	b	ϵ'_f	c
3,967E-03	2609	0,32	-0,07	22	-0,59

Table 5: Hypothesis Cycle between 20°C-T_{MAX} and 20°C-T_{MIN}

5.2 Worst Case

$\Delta\varepsilon/2$	N_f	σ'_f/E	b	ε'_f	c
4,372E-03	1987	0,32	-0,07	22	-0,59

Table 6: Hypothesis Cycle from zero

5.3 Realistic Case

Table 7: Hypothesis Cycle between 20°C-T_{MAX} and getting cold until T_{MIN}

As it is possible to see from tables, in all cases there is the respect of Normative Fiat 7-A3760. In fact, obtained results are fatigue breaking numbers (N_f) greater than 1000 cycles.

6 Discussion and Conclusions

Simulative tests with F.E.M. can be utilized to substitute experimental tests, as in this work. In fact obtained results are in according to experimental results. Extreme cases, the best and worst cases, determine, respectively, maximum and minimum security. In best case there is a great security range: in fact $N_f = 2609 > 1000$. Also in worst case there is the respect of normative, with $N_f = 1987 > 1000$. But the credible result is in the realistic case, with $N_f = 2200 > 1000$, when it images *hot end* increases its temperature by 20° (environmental temperature) until T_{MAX} and after there is a unloaded material, that gets cold until T_{MIN}. With this procedure is possible to save time and money, obtaining results very near to reality and making a comparison with experimental data.

References:

- [1] "Norma di sperimentazione 7 – A3760", FIAT AUTO S.P.A., Novembre (1998).
- [2] C. Hoffman, *An investigation of high temperature low cycle fatigue behaviour of materials*, Ph.D. dissertation, University of Connecticut (1982).
- [3] D. T: Raske and J. Morrow, *Mechanics of materials in low cycle fatigue testing*, Manual on Low Cycle Fatigue Testing, ASTM STP 465, (1969), pp. 1-25.
- [4] J. F. Tavernalli and L. F: Coffin, *A compilation and interpretation of cyclic strain fatigue tests on metals*, Trans. ASM 51, (1959), 438-450.
- [5]; L. F. Coffin, *The effect of high vacuum on the low cycle fatigue law*, Metall. Trans.3, (1972), 1777-1788.
- [6] W. B. Jones, *The effects of mechanical cycling on the substructure of modified 9Cr-1Mo ferritic steel. In Ferritic Steels for High*

Temperature Applications (Edited by Khare A. K.), American Society for Metals, (1983), pp. 221-235.

- [7] R. C. Boettner, C. Laird and A. J. McEvily, *Crack nucleation and growth in high strain-low cycle fatigue*, Trans. Metall. Soc. AIME 233, (1965), 379-387.
- [8] A. J. McEvily, *On the quantitative analysis of*

$\Delta\varepsilon/2$	N_f	σ'_f/E	b	ε'_f	c
4,214E-03	2200	0,32	-0,07	22	-0,59

fatigue crack propagation. Fatigue Mechanisms: Advances in Quantitative Measurement of Physical Damage, ASTM STP 811, (1982), pp. 283-312.

- [9] B. A. Bilby, A. H. Cottrell and K.H. Swinden, *The spread of plastic yield from a notch*, Proc.R. Soc. Lond. A 271, (1963), 304-310.
- [10]P. Neumann *Coarse slip model of fatigue*, Acta metall. 17, (1969), 1219-1225.
- [11]B. Tomkins and W.D. Biggs *Low endurance fatigue in metals and polymers*, J.Mater. Sci. 4, (1969), 544-553.
- [12]Hyper Mesh 5.0, "Quick Reference Guide" , 1998.
- [13] M. Reymond & M. Miller, "MSC/NASTRAN 70.7, Quick Reference Guide, version 70" , 1994